Supplement of The Cryosphere Discuss., 9, 4019–4042, 2015
http://www.the-cryosphere-discuss.net/9/4019/2015/
doi:10.5194/tcd-9-4019-2015-supplement

The Cryosphere
Discussions
Open Access

Supplement of

Tropical and mid-latitude forcing of continental Antarctic temperatures

C. S. M. Turney et al.

Correspondence to: C. S. M. Turney (c.turney@unsw.edu.au)

Text S1: 2012 South Geographic Pole core

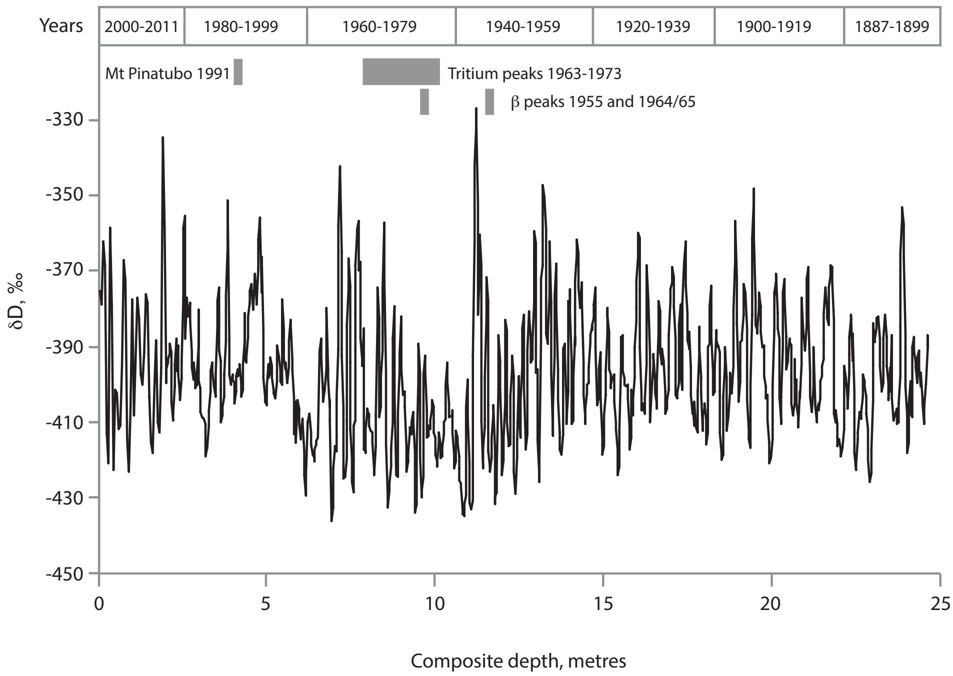

Figure S1: South Geographic Pole δD values on common depth scale with chronology, compiled from present study and previous work (Jouzel et al., 1983). Independent checks on chronology are provided by the tropical 1991 eruption of Mount Pinatubo and/or the Cerro Hudson (identified by a prominent non-sea salt sulfate peak) and known tritium and β peaks.

Text S2: Spatial Controls on Antarctic Warming

The same relationship observed between the surface pressure anomalies and temperature extends up to 700 hPa (Figure S2).

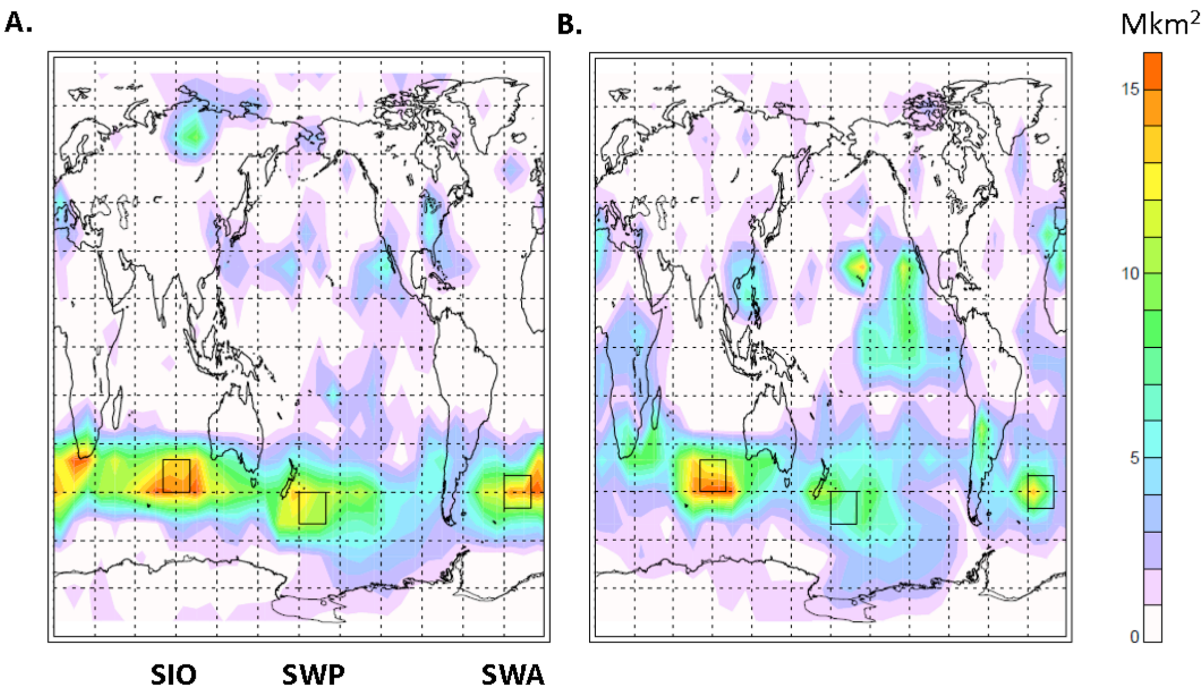

Figure S2: Panel A. The cumulative area of significant positive 700 hPa temperature anomalies poleward of 65˚S (in million km^2) produced by compositing months having negative 700 hPa geopotential height anomalies (thresholded at the 10^{th} percentile) in each 10˚ x 10˚ (longitude x latitude) box, obtained from deseasonalised monthly ERA-Interim reanalysis data for 1979-2012 (Dee et al., 2011). The three boxes define the positions referred to in the text as Southern Indian Ocean (SIO), Southwestern Pacific (SWP) and Southwestern Atlantic (SWA). Panel B. shows the opposite relationship i.e. the area of negative 700 hPa temperature anomalies produced by compositing months of positive 700 hPa geopotential height anomalies (thresholded at the 90^{th} percentile). The grid spacing is 15˚ in longitude and latitude. For reference, the area of the Antarctic continent is 14 million km^2 and the area poleward of 65˚S is 25 million km^2.

Applying the analysis used for Figures 4 and S2, we show in Figure S3 panel A (B) the area of significant positive (negative) surface pressure anomalies south of 65˚S that is associated with positive (negative) surface pressure anomalies in each grid box. The strongest association with Antarctic surface temperature anomalies is from pressure anomalies of the same sign within the Antarctic region, which is distinctly different to the association shown in Figure 4. Associations with the key centres shown in Figure 4 are largely absent.

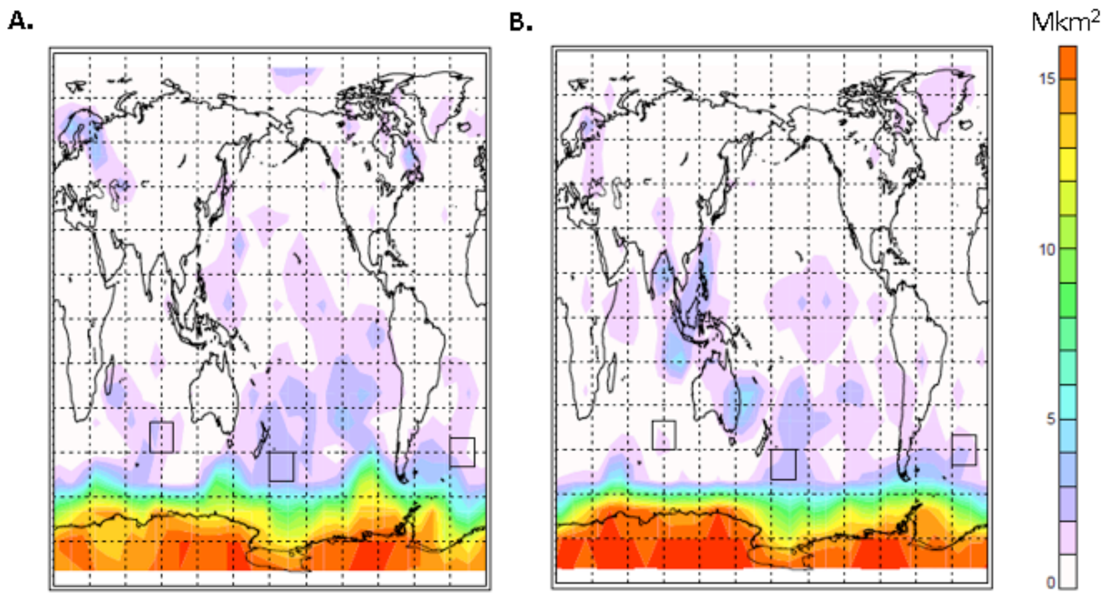

Figure S3: Panel A. The cumulative area of significant positive surface temperature anomalies poleward of 65˚S (in million km^2) produced by compositing months of positive surface pressure anomalies (thresholded at the 10^{th} percentile) in each 10˚ x 10˚ (longitude x latitude) box, obtained from deseasonalised monthly ERA-Interim reanalysis data for 1979-2012. Panel B. shows the opposite relationship i.e. the area of negative temperature anomalies produced by compositing months of negative surface pressure anomalies (thresholded at the 90th percentile). The grid spacing is 15° in longitude and latitude.

Text S3: Temperature Relationships with Zone Wave 3 Centres

Composites were formed for deseasonalised sea level pressure (SLP) anomalies averaged over the southern Indian Ocean (SIO) and southwestern Pacific (SWP) regions identified in Figure 2 for deseasonalised values of surface temperature, zonal and meridional wind speed, vertical pressure wind and geopotential height. Figures 6 and S4 relate to the SIO region using ERA-Interim and 20CR reanalysis, respectively, while Figures 7 and S5 relate to the SWP region for ERA-Interim and 20CR reanalyses, respectively. SLP anomalies were formed from each respective reanalysis with respect to the 1979-2012 base period.

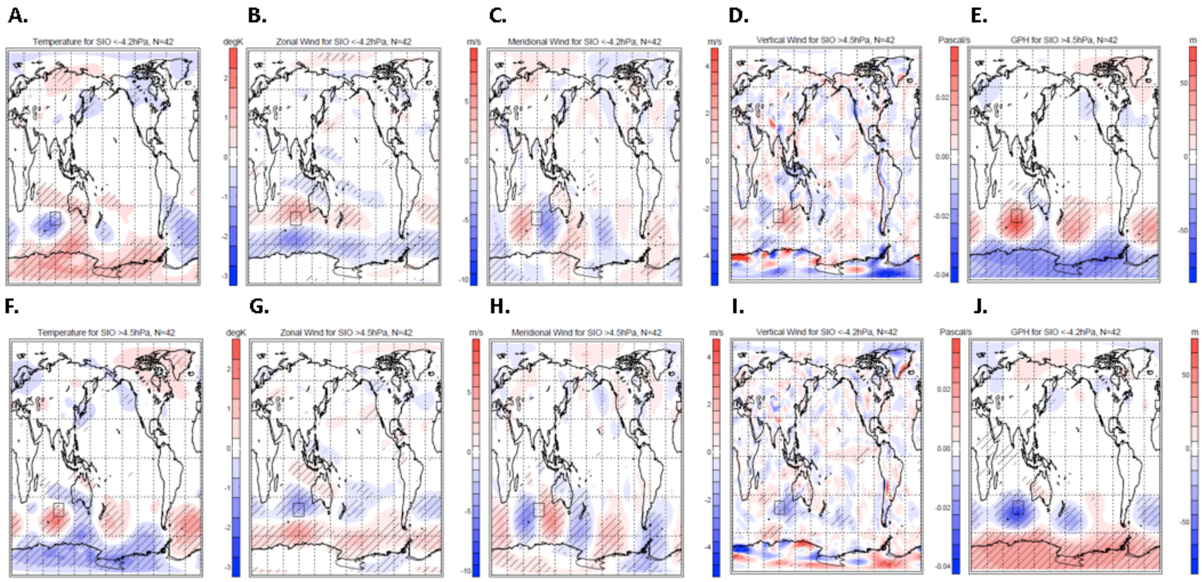

Figure S4: Composites of deseasonalised monthly 20CR reanalysis fields at 700 hPa for surface pressure 10th percentile (negative) and 90th percentile (positive) anomalies in the southern Indian Ocean (SIO) (80-100˚E, 35-45˚S) for 1979-2012. Shown are temperature (A. and F.), zonal wind speed (B. and G.; positive = eastward) and meridional wind speed (C. and H.; positive = northward), vertical pressure wind (D. and I.; positive = downward) and geopotential height (E. and J.). The SIO surface pressure anomaly threshold and the number of months (N) contributing to each composite are shown at the top of each panel. Hatched areas denote areas of statistical significance (95% confidence).

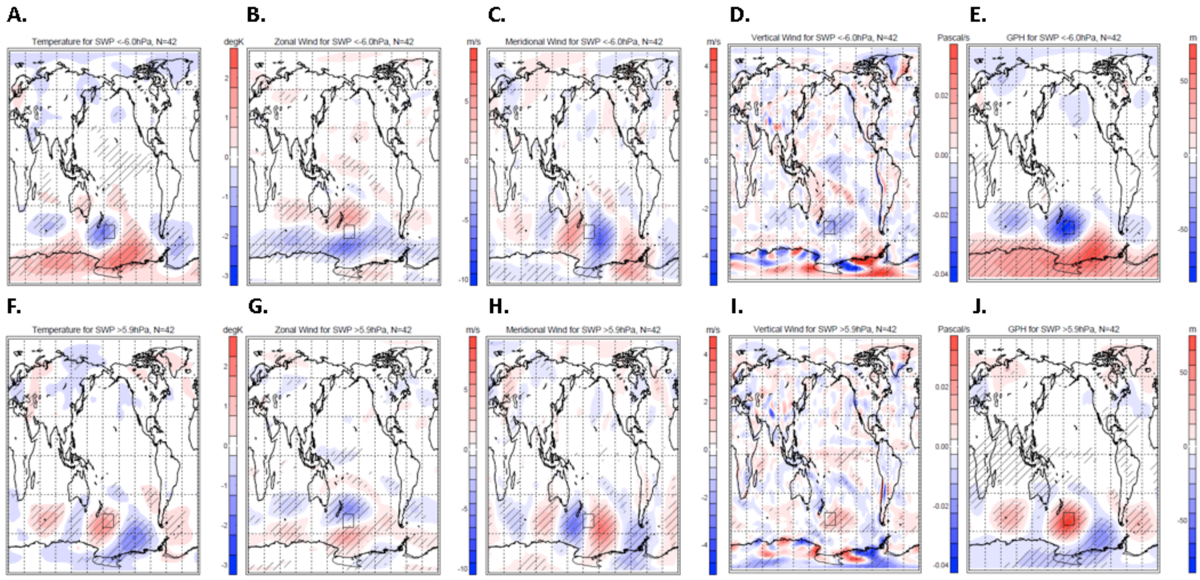

Figure S5: Composites of deseasonalised monthly 20CR reanalysis fields at 700 hPa for surface pressure 10th percentile (negative) and 90th percentile (positive) anomalies in the southwestern Pacific (SWP) Ocean (180-200˚E, 45-55˚S) for 1979-2012. Shown are temperature (A. and F.), zonal wind speed (B. and G.; positive = eastward) and meridional wind speed (C. and H.; positive = eastward), vertical pressure wind (D. and I.; positive = downward) and geopotential height (E. and J.). The SWP surface pressure anomaly threshold and the number of months (N) contributing to each composite are shown at the top of each panel. Hatched areas denote areas of statistical significance (95% confidence).

Text S4: Overturning Circulation and Tropical Teleconnections

We considered the influence of the surface pressure anomalies on the structure of the overturning circulation by examining the meridional mass streamfunction. Figure 8 shows composites of the deseasonalised zonal mean streamfunction poleward of 15˚S for negative, positive and intermediate surface pressure anomalies in the SIO and SWP regions. Generally, in comparison for the situation in the intermediate state, the negative anomaly state shows a weakening (reduced volume) of the Polar cell and a strengthening (increased volume) of the Ferrel cell (particularly on the poleward side of the cell), which is consistent with increased poleward heat transport. For the positive anomaly in comparison with the intermediate state, the Polar cell appears slightly strengthened in the case of anomaly in the SIO region, while the Ferrel cell appears slightly weaker in the case of the anomaly in the SWP region. While less clear, the circulation changes in the positive state are consistent with reduced poleward heat transport.

References

Dee, D. P., Uppala, S. M., Simmons, A. J., Berrisford, P., Poli, P., Kobayashi, S., Andrae, U., Balmaseda, M. A., Balsamo, G., Bauer, P., Bechtold, P., Beljaars, A. C. M., van de Berg, L., Bidlot, J., Bormann, N., Delsol, C., Dragani, R., Fuentes, M., Geer, A. J., Haimberger, L., Healy, S. B., Hersbach, H., Hólm, E. V., Isaksen, L., Kållberg, P., Köhler, M., Matricardi, M., McNally, A. P., Monge-Sanz, B. M., Morcrette, J. J., Park, B. K., Peubey, C., de Rosnay, P., Tavolato, C., Thépaut, J. N., and Vitart, F.: The ERA-Interim reanalysis: configuration and performance of the data assimilation system, Quarterly Journal of the Royal Meteorological Society, 137, 553-597, 2011.

Jouzel, J., Merlivat, L., Petit, J. R., and Lorius, C.: Climatic information over the last century deduced from a detailed isotopic record in the South Pole snow, Journal of Geophysical Research, 88, 2693-2703, 1983.